Engineering momentum profiles of cold-atom beams

D Hudson Smith[1] and Artem G Volosniev[2]
[1] *Clemson University, Clemson, South Carolina 29634, USA*
[2] *Institut für Kernphysik, Technische Universität Darmstadt, 64289 Darmstadt, Germany*
(Dated: January 7, 2019)

We ...

INTRODUCTION

Scattering is one of the most important observational tools in science. In physics, it is used in almost all subfields to understand internal structure of particles, materials, structures (cite).

In systems of cold atoms scattering might seem obsolete because the energies are so low that usually only a few parameters determine physics, i.e., the system is in a universal regime. However, even at these low temperatures observables can strongly depend on the incoming momentum (see Figure 1a). For example, ...

Figure 1a: examples where observables depend strongly on the incoming momentum: time-dependent one- and two-body scattering, three-body recombination, polaron. Figure 1b: a sketch of the set-up for engineering beams with desirable momentum profiles: two reservoirs and a link between them.

Here we study how to create fluxes with cold atoms, which can be used to study systems of cold atoms in scattering experiments. We illustrate using the one-dimensional Bose polaron problem.

DESIGN

Physical System

Describe the system. The system has three parts: Two reservoirs and a link between them; see Figure 1a. One reservoir is made of a non-interacting (for simplicity) gas of particles at temperature T. We call these particles probes or A. The reservoir is connected to the link. The link is a potential that acts only on particles A (for simplicity). The second reservoir is made of interacting particles B. These particles make a system of interest, which we would like to analyze.

Procedure for Finding a Link Potential

We find an appropriate link potential $V_0(x) \equiv V(x, \boldsymbol{\theta}^*)$ by performing a global search over a family of possible potentials $V(x, \boldsymbol{\theta})$ for the parameters $\boldsymbol{\theta}^*$ that reduce the k-integrated squared error between the desired transmission-momentum profile $T_0(k)$ and the actual profile $T_{\boldsymbol{\theta}}(k)$ determined by a sample potential $V(x, \boldsymbol{\theta})$. Concretely, we minimize the cost

$$J_{\boldsymbol{\theta}} = \sum_k w_k \left| T_0(k) - T_\theta(k) \right|^2, \tag{1}$$

where the k-integral has been approximated (up to a constant factor) by a sum over a discrete set of momentum values, and w_k is the weight given to momentum k. The weights are chosen to emphasize regions of k during the minimization. For instance, when trying to create a "comb" potential that forbids transmission for all k except in the neighborhood of a chosen value k_0, then it would be appropriate to increase the weights in the region of k_0. We find that results are sensitive to the choice of w_k, and some trial and error was required to get acceptable potentials.

With the goal of discovering experimentally viable solutions, we parameterize the family of link potentials $V(x, \boldsymbol{\theta})$, as a sum of N Gaussian potentials each of the form

$$V_i(x; A_i, \mu_i, \sigma_i) = \frac{A_i}{\sqrt{2\pi\sigma_i^2}} \exp\left[-\frac{(x-\mu_i)^2}{2\sigma_i^2} \right], \tag{2}$$

While minimizing Eq. (1), we enforce the parameter constraints listed in Table I. In addition to these explicit constraints on the parameters, we enforce an implicit constraint by requiring that the link potential should not extend beyond the region of potential support $x \in [-x_0, x_0]$. To accomplish this, we minimize the augmented cost

$$J^{\text{aug}}_{\boldsymbol{\theta}} = J_{\boldsymbol{\theta}} + \alpha \sum_i^N \int_{|x|>x_0} dx \, |V_i(x; A_i, \mu_i, \sigma_i)|^2, \tag{3}$$

where α is a tuning parameter chosen to make the added term of a similar order to J_θ in the scenario that the potential extends outside the support region. Beyond this, we find that results are not very sensitive to the choice of α probably due to the very short tails of the Gaussian potentials. The integral in Eq. (3) evaluates to the complementary error function. The full form is given in the suppl. material.

For a choice of $\boldsymbol{\theta}$ (and hence $V(x; \boldsymbol{\theta})$), we solve for $T_{\boldsymbol{\theta}}(k)$ by integrating Schrödinger's equation across the region of the potential and calculating the ratio of the transmitted to the incident flux. In order to do this efficiently, we approximate the integral as a banded linear

Constraints	Experimental Rationale
$\sum_{i=1}^{N} \mu_i = 0$	The cost function has a continuous degeneracy associated with overall translations of the link potential.
$\sigma_{\min} \leq \sigma_j \leq \sigma_{\max}$	Laser beam widths fall between a minimum and maximum value.
$A_{\min} \leq \lvert A_j \rvert \leq A_{\max}$	Laser amplitudes fall between a minimum and maximum value.

TABLE I: The explicit constraints on the potential parameters and the rationale for each constraint. The values of $\sigma_{\min}$, $\sigma_{\max}$, $A_{\min}$, and $A_{\max}$ must be determined from the experimental context.

system of equations solvable in $O(M)$ time where M is the number of x-steps. Using these techniques we are able to evaluate the transmission coefficient x thousand times per second on a 7th generation Intel Core i7 processor under the conditions used in our tests.

We minimize $J_{\boldsymbol{\theta}}^{\text{aug}}$ for $\boldsymbol{\theta}^*$ using the global optimization routine called Differential Evolution (DE) [**?**]. This evolutionary-based search algorithm is suitable given the non-convex (multiple local minima) nature of the optimization problem. Despite its simplicity, DE does a good job of balancing exploration of the space of link potentials against the need to efficiently learn from each sample with little tuning of the model settings. Emperically, we found DE to perform much better than several other approaches including random search, Nelder-Mead, and Simulated Annealing [**?**].

Single-comb transport profile

To illustrate the method described above we optimize for a single-comb transport profile sharply-peaked near $k = 1$ ($\hbar = 2m = 1$). For our target transport profile, we use a Lorentz distribution peaked at $k = 1$ and with a small HWHM (see Figure 1, top). For the constraints shown in Table I, we use $\sigma_{\min} = 0.X$, $\sigma_{\max} = Y.Y$, $A_{\min} = 0.X$, and $A_{\max} = Y.Y$. We simplify the optimization by searching over two-Gaussian link-potentials with equal amplitudes and widths. The resulting optimization has three parameters. Despite the few parameters, the cost function for this optimization has many local minima corresponding to the many ways that a resonance state can be placed near the scattering energy k^2. So, while this is a very simple example, it still requires a method for globally searching the space of link potentials.

Figure 1 shows the link potential and transport profile resulting for the single-comb optimization. The solution does a good job of suppressing transport except near $k = 1$ as set by our Lorentz target profile and near $k = 2$ resulting from a second resonance in the scattering potential. This additional resonance need not be a problem if the scattering atoms are sourced from a thermal reservoir with sufficiently low population near $k = 2$. The two-Gaussian solution struggles to reproduce the width of the Lorentz target profile (see inset). Though we have not demonstrated that the solution shown in Fig. 1 corresponds to a global minimum, this failure to reproduce the width may result from insufficient freedom in the family of constrained two-Gaussian potentials.

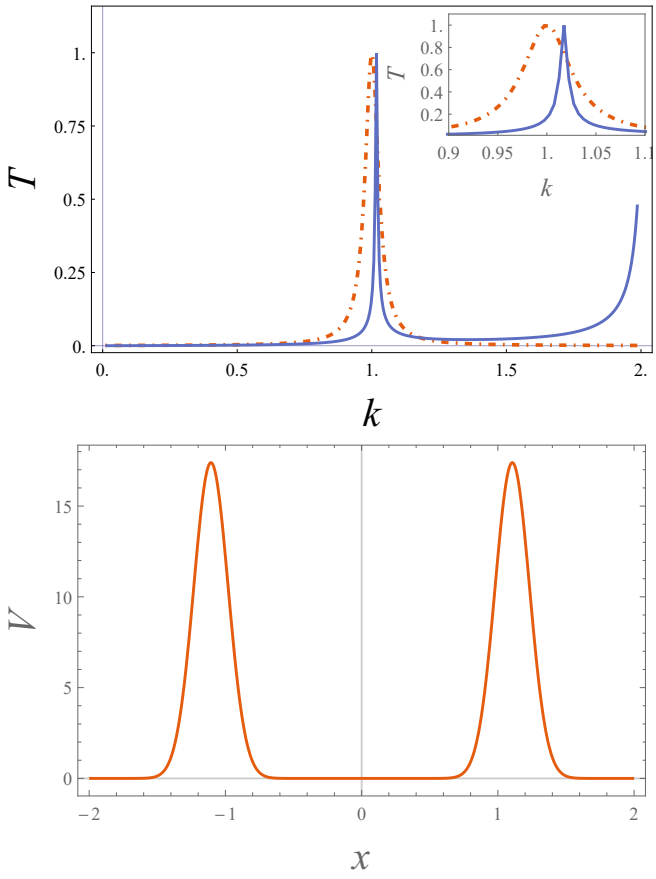

FIG. 1: Two-Gaussian solution for the $k = 1$ comb transport profile. The top figure shows the target profile (dot-dashed, red) used during optimization and the actual profile resulting from the optimization procedure. The inset is a zoomed-in view of the region around the peak near $k = 1$. The bottom figure shows the optimal link potential $V(x)$.

It may be experimentally problematic if the transport profile shown in Figure 1 were highly sensitive to the potential parameters. Such sensitivity would require extremely fine control over the laser amplitudes, positions, and widths in order to produce the desired potential. To test this sensitivity, we generate 200 perturbed potentials by varying the six parameters of the two-Gaussian solution shown in Fig. 1 by a random-normal multiplicative factor with mean 1 and standard deviation 0.05. The distributions of the peak positions and heights for the 200

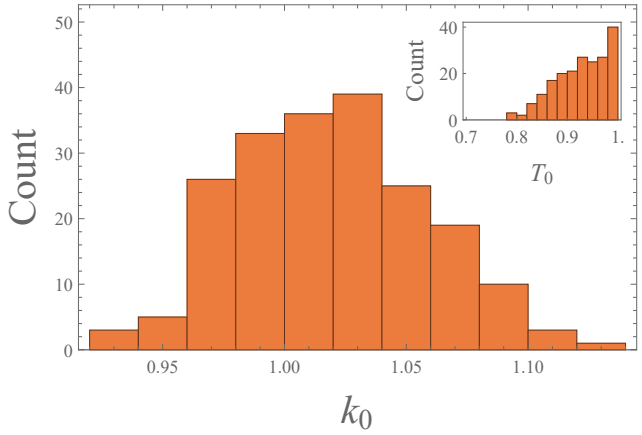

FIG. 2: Sensitivity of the transport profile to perturbations of the potential parameters. Shown are the distributions of the peak position k_0 (main graph) and peak height T_0 (inset) for 200 potentials with parameters randomly perturbed on the order of 5% from the optimized potential shown in Fig. 1.

perturbed potentials are shown in Figure 2. Both the peak positions, k_0, and the peak heights, T_0, undergo perturbations on the scale of the 5% potential perturbations suggesting that transport properties are relatively insensitive to slight errors in the potential parameters. When optimizing with 3- or 4-Gaussian potentials, we found that solutions tended to be extremely sensitive to the potential parameters. If such potentials are needed to produce the desired transport profile, it may be possible to further augment the cost function in order to preference solutions that are less sensitive to potential perturbations.

Though we have demonstrated our optimization method in a very simple scenario, it is possible to apply this technique to more complicated scenarios such as double-comb or step transport profiles for various experimental scenarios. We find that these more complicated transport profiles require more than two Gaussian potentials and that the solutions using the procedure we describe are highly-sensitive to the potential parameters. We leave the thorough exploration of these ideas to future work. In the next section, we discuss a possible experimental application of the single-comb solution.

ILLUSTRATION

The Bose polaron problem is very interesting, and many groups are studying it now. It is an open question how to measure the effective mass of the impurity in one-dimensional set-ups. There was one experiment, however the results are unclear. Also it is interesting to understand when the model breaks, i.e., at which momenta. We propose the following experiment: One reservoir – probes, the link is from Fig. 2 (comb), the second reservoir is an interacting homogeneous Bose gas (for simplicity). Provide some realistic numbers. Probably some simple calculations (in the suppl. material).

Figure 3: Bose polaron set-up. Measurement of the effective mass – the change of the energy upon interaction change.

SUMMARY

We have shown how to create beams of particles to probe systems of cold atoms. We have illustrated the idea using the Bose polaron problem. Other interesting examples include ...

We thank Michael Fleischhauer for referring to [**?**]. A. G. V. gratefully acknowledges the support of the Humboldt Foundation.

SUPPLEMENTARY MATERIAL

POLARON

To model one impurity atom that moves through the one-dimensional environment made of N cold bosonic atoms, we employ the following Hamiltonian

$$H = -\frac{\hbar^2}{2m}\sum_{i=1}^{N}\frac{\partial^2}{\partial x_i^2} - \frac{\hbar^2}{2M}\frac{\partial^2}{\partial y^2} + g\sum_{i>j=1}^{N}\delta(x_i - x_j) + c\sum_{i=1}^{N}\delta(x_i - y), \tag{4}$$

where M is the mass of the impurity atom, and m is the mass of a bosonic particle. The position of the impurity is y, bosons are described by the set of coordinates $\{x_i\}$. We assume that the realistic boson-boson and boson-impurity interactions are well-described by the zero-range potentials of strengths g and c respectively. The reservoir by assumption is large, such that the dynamics can be described by the thermodynamic limit $N \to \infty$ assuming a certain value of the density ρ. To take the thermodynamic limit we set the periodic boundary conditions: The

particles move in a ring of the circumference L, such that $0 < x_i < L$ and $0 < y < L$. This assumption is not essential for our problem, because we are interested in the limit $N(L) \to \infty$ with $\rho = \frac{N}{L}$.

Every eigenfunction of the Hamiltonian can be written as $\Psi = \sum_{\{n_j\},m} a_{\{n_j\},m} e^{2\pi i \frac{\sum n_j x_j + m y}{L}}$. Because all interactions are pairwise, the total (angular) momentum of the system must be conserved, and we write it as $P = \frac{2\pi\hbar}{L}\left(\sum_j n_j + m\right)$. Since we have a conserved quantity (P), we may exclude the coordinate of the impurity from the consideration. To this end, we write the function Ψ as $\Psi = e^{i\frac{Py}{\hbar}} \sum_{\{n_j\},m} a_{\{n_j\},m} e^{2\pi i \frac{\sum n_j z_j}{L}} \equiv e^{i\frac{Py}{\hbar}} \psi(z_1, ..., z_N)$ with $z_i = L\theta(x_i - y) + x_i - y$, where $\theta(x)$ is the Heavyside step function, i.e., $\theta(x > 1) = 1$ and zero otherwise. The variables z_i are defined such that $0 \le z_i \le L$ and the impurity is placed at $z = 0$ and $z = L$. Now if we insert this function into the Schrödinger equation, $H\Psi = \mathcal{E}\Psi$, we obtain the following equation for $\psi(0 < z_i < L)$

$$-\frac{\hbar^2}{2m}\sum_i \frac{\partial^2\psi}{\partial z_i^2} - \frac{\hbar^2}{2M}\left(\sum_i \frac{\partial\psi}{\partial z_i}\right)^2 + i\frac{\hbar P}{M}\sum_i \frac{\partial\psi}{\partial z_i} + g\sum_{i>j}\delta(z_i - z_j)\psi = \left(\mathcal{E} - \frac{P^2}{2M}\right)\psi, \tag{5}$$

which must be supplemented with the boundary conditions:

$$\psi(z_i = 0) = \psi(z_i = L); \qquad \left.\frac{\partial\psi}{\partial z_i}\right|_{z_i=L^-}^{z_i=0^+} = \frac{2c\kappa}{\hbar^2}\psi(z_i = 0), \tag{6}$$

where $\kappa = mM/(m + M)$ is the reduced mass.

By assumption the bosons are weakly-interacting, therefore we use the ansatz $\psi = \prod_i \Phi(z_i)$ to approximate the function. To minimize the expectation value of the Hamiltonian the function $\Phi(z)$ must satisfy the following Gross-Pitaevski-type equation

$$-\frac{\hbar^2}{2\kappa}\frac{\partial^2\Phi}{\partial z^2} + i\frac{\hbar P}{M}\frac{\partial\Phi}{\partial z} - i\frac{\hbar^2(N-1)A}{M}\frac{\partial\Phi}{\partial z} + g(N-1)|\Phi|^2\Phi = \mu\Phi, \tag{7}$$

where $A = -i\int \Phi(x)^* \frac{\partial}{\partial x}\Phi(x)\mathrm{d}x$ defines the momentum of a boson, and μ is the chemical potential (it appears as the Lagrange multiplier). We rewrite this equation as

$$-\frac{\partial^2\Phi}{\partial z^2} + iv\frac{\partial\Phi}{\partial z} + \tilde{g}(N-1)|\Phi|^2\Phi + \tilde{c}\delta(z)\Phi = \tilde{\mu}\Phi, \tag{8}$$

where $\tilde{\mu} = \frac{2\kappa\mu}{\hbar^2}$, $\tilde{g} = \frac{2\kappa g}{\hbar^2}$, $\tilde{c} = \frac{2\kappa c}{\hbar^2}$ and $v \equiv \frac{2\kappa P_I}{M\hbar}$, where $P_I = P - \hbar A(N-1)$ defines the momentum of the impurity in the thermodynamic limit. Note the corresponding boundary conditions

$$\Phi(z = 0) = \Phi(z = L); \qquad \left.\frac{\partial\Phi}{\partial z}\right|_{z=L^-}^{z=0^+} = \tilde{c}\Phi(0), \tag{9}$$

This non-linear equation (8) has an analytic solution for the soliton-like behavior [**?** **?**], which determines the properties of the polaron in our problem. Let us first consider the case with $c = 0$. In this case the solution for $v > 0$ is

$$\Phi = \sqrt{\frac{\tilde{\mu}}{\tilde{g}(N-1)}}\left(1 - \beta\,\mathrm{sech}^2\left[\sqrt{\frac{\tilde{\mu}\beta}{2}}(z + z_0)\right]\right)^{\frac{1}{2}} e^{i\phi(z)}, \tag{10}$$

$$\phi(z) = -\pi\theta(z + z_0) + \arctan\left(\frac{\sqrt{\frac{2v^2}{\tilde{\mu}}\beta}}{\exp\left[\sqrt{2\tilde{\mu}\beta}(z + z_0)\right] - 2\beta + 1}\right), \tag{11}$$

where $\beta = 1 - v^2/(2\tilde{\mu})$, and z_0 is some parameter that should be determined from the boundary conditions. It is worthwhile noting that the solution for $v < 0$ is Φ^*. We plot this solution in Figs. 3 and 4; for simplicity we consider the region $-L/2 < z < L/2$, the region $0 < z < L$ easily follows. Note that the solution is not periodic (see ϕ), however by combining two solution with $\pm z_0$ we can construct a periodic solution with a singularity at $z = 0$. Therefore, the polaron in this picture is a combination of two moving solitons: The impurity creates a topological defect, which leads to a quasiparticle picture.

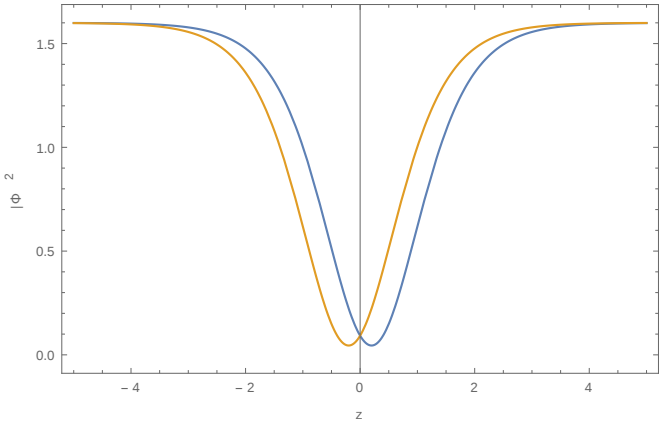

FIG. 3: The density, $|\Phi|^2$, of the Bose gas for two different parameters z_0: $z_0 = 0.2$ (left curve), $z_0 = -0.2$, assuming that $\tilde{\mu} = 1.6, v = 0.3$ (everything in arbitrary units). Note that the minimum of the density is at $-z_0$.

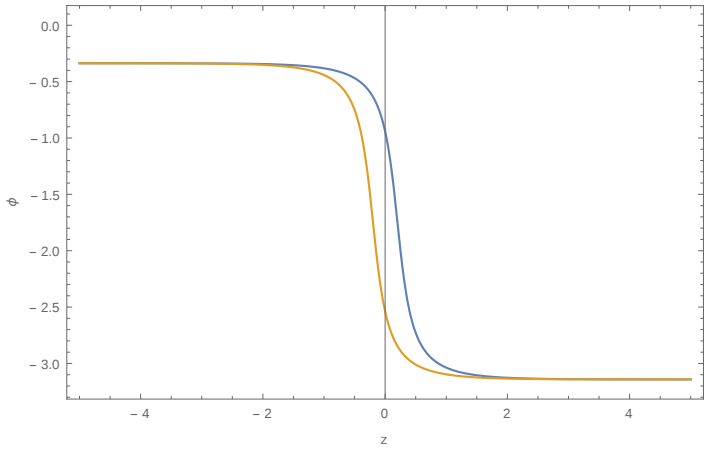

FIG. 4: The phase, ϕ, of the Bose gas for two different parameters z_0: $z_0 = 0.2$ (left curve), $z_0 = -0.2$, assuming that $\tilde{\mu} = 1.6, v = 0.3$ (everything in arbitrary units).

We write the wave function for the polaron as

$$\Phi = \sqrt{\frac{\tilde{\mu}}{\tilde{g}(N-1)}} \left(1 - \beta \mathrm{sech}^2 \left[\sqrt{\frac{\tilde{\mu}\beta}{2}}(z \pm z_0)\right]\right)^{\frac{1}{2}} e^{i\phi(z)}, \tag{12}$$

with

$$\phi(z) = \delta\phi\theta(-z) + \arctan\left(\frac{\sqrt{\frac{2v^2}{\tilde{\mu}}\beta}}{\exp\left[\sqrt{2\tilde{\mu}\beta}(z \pm z_0)\right] - 2\beta + 1}\right), \tag{13}$$

where the parameter $\delta\phi$ is not important for the further derivations, it reassures that the function is periodic (in the thermodynamic limit it is written as $2\pi - \arctan\left[\frac{\sqrt{\frac{2v^2}{\tilde{\mu}}\beta}}{1-2\beta}\right]$); the plus sign in $\pm$ corresponds to $z > 0$ and the minus sign to $z < 0$. The wave function can be easily visualised from Figs. 3 and 4. The density has a non-analytic derivative at $z = 0$. The phase is discontinuous function at $z = 0$ (the derivative is continuous).

The corresponding chemical potential is found from the normalization condition $\int \Phi^2 = 1$, for large values of N and L it reads

$$\tilde{\mu} = \gamma\rho^2 \frac{N-1}{N}\left(1 - 2\sqrt{2\beta}\frac{(\tanh(d) - 1)}{\sqrt{\gamma}N}\right), \tag{14}$$

where $\rho = N/L$, $\gamma = \tilde{g}/\rho$, and $d = \sqrt{\frac{\gamma\beta}{2}}\rho z_0$. The condition on z_0 is found by using the boundary conditions at $z = \{0, L\}$

$$\frac{\tilde{c}}{\rho\sqrt{2\gamma}} = \frac{\beta^{\frac{3}{2}}\tanh(d)}{-\beta + \cosh^2(d)}. \tag{15}$$

This equation is cubic (in $\tanh(d)$), hence, the solutions can be found in a closed form. Now we can calculate the energy of the polaron in the thermodynamic limit

$$E \equiv \lim_{N\to\infty, \frac{N}{L}\to\rho} \left[\mathcal{E}(c, P) - \mathcal{E}(c = 0, P = 0)\right], \tag{16}$$

where

$$\mathcal{E}(c, P) = \frac{P^2}{2M} + \mu N - \frac{\hbar^2 A^2 N(N-1)}{2M} - gN(N-1)\int_0^{L/2} |\Phi|^4 \mathrm{d}z. \tag{17}$$

Using these expressions we derive

$$E = \frac{P_I^2}{2M} + \frac{\hbar^2\rho}{2\kappa}\frac{\sqrt{2\tilde{g}\rho\beta}}{3}\left[4b + (-4b + \beta\mathrm{sech}^2(d))\tanh(d)\right] + \frac{\hbar P_I}{M}\lim_{N\to\infty} AN, \tag{18}$$

where $b = 1 + \frac{v^2}{4\tilde{g}\rho} = 1 + \frac{\kappa P_I^2}{2M^2 g\rho}$. This energy for $v \to 0$ can be written as

$$E \simeq \epsilon + \frac{P_I^2}{2m_{\text{eff}}}, \tag{19}$$

where ϵ is the effective energy of the polaron, and m_{eff} is the effective mass.

Further Discussions in the supplementary material and in the paper:
Discuss the effective mass.
Discuss the two different solutions.
Discuss the critical momentum.
Discuss the quench dynamics to the polaron.
Discuss the literature.

Cost Function

$$J'_\theta = J_\theta + \alpha J_{\text{boundary}}, \tag{20}$$

where $\alpha > 0$ is the weight given to cost incurred for having the potential extend outside the support region of the potential.